Proceedings of the 1992 IEEE/RSJ International Conference on Intelligent Robots and Systems Raleigh, NC July 7-10, 1992

Grasp Recognition Using the Contact Web

Sing Bing Kang and Katsushi Ikeuchi

The Robotics Institute
Carnegie Mellon University
Pittsburgh, PA 15213

Abstract - **We propose an approach to teach robots to perform grasping tasks. This approach is based on the Assembly Plan from Observation (APO) paradigm, where the key idea is to enable a system to observe a human performing a grasping task, understand it, and perform the task with minimal human intervention.**

A grasping task is composed of three phases: pre-grasp phase, static grasp phase, and manipulation phase. The first step in recognizing a grasping task is to identify the grasp itself (within the static grasp phase).

We propose to identify the grasp by means of a grasp representation called the *contact web* which is composed of a pattern of effective contact points between the hand and the object. We also propose a grasp taxonomy based on the contact web to systematically identify a grasp. Results from grasping experiments show that it is possible to distinguish between various types of grasps using the proposed contact web and grasp taxonomy.

1.0 Introduction

Robot programming is an essential component of task automation. The current methods for robot programming include teaching (e.g., [1], [2]), textual programming (e.g., [3]), and automatic programming (e.g., [4], [6]). The first two methods are by far the most pervasive in both the industrial and academic environments. In teaching methods, the robot or manipulator learns its trajectory either through a teach pendant or actual guidance through the sequence of operations ("teach-by-guiding" or less appropriately "teach-by-showing"). Textual programming, while flexible, requires expertise and often a long development time. Several of the robot programming languages include AL, AML, RAIL, RPL, and VAL. In automatic programming, the only inputs required to generate the control command sequences to the robot system are the description of the objects involved in the task and the high-level task specifications. However, realization of a practical system with automatic programming is difficult because of problems in optimal grasp generation, path-planning and the translation from high-level goals to lower level commands.

We could reduce the severity of such problems by using a different approach to task programming. We are particularly interested in programming the robot to perform grasping tasks. The analysis of grasps and their purposes is important because most tasks performed by humans, especially manufacturing tasks [12], involve grasping. Automation of tasks would almost certainly involve analysis of grasps.

The ideas and goals of our work are based on those embodied in the Assembly Plan from Observation (APO) paradigm proposed by Ikeuchi and Suehiro [5]. They describe a system that observes a human performing an assembly task while a geometric reasoner analyzes and recognizes the task from observation, and generates the same assembly sequence for a robot. In this paradigm, the human operator does all the thinking - the system "understands" what needs to be done based on what is observed and performs the task or tasks. A similar approach was taken by Kuniyoshi et al. [6] who developed a system which emulates the performance of a human operator. However, their system is restricted to pick-and-place operations.

This paper is an account of our work on grasp identification. In Section 2, we describe a 3-D structure called the *contact web* which can be used to classify a grasp. It also facilitates higher level descriptions of a grasp by using an objective function. The grasp recognition procedure is delineated in Section 3. We summarize our findings in Section 4.

2.0 Grasp Identification

Grasp identification is central to the recognition of grasping tasks. In order to identify grasps, we need a suitable grasp taxonomy.

2.1 Classification of Grasps

There has been a lot of study in the medical community on the grasping capabilities of the human hand, from both the anatomical and functional points of view. Schlesinger [10] and Taylor and Schwarz [9] associate human grasps primarily with the object shape in their categorization of six grasps (cylindrical, fingertip, hook, palmar, spherical and lateral).

Napier [17], on the other hand, dichotomized grasps into precision grasps and power grasps. His classification of grasps

0-7803-0737-2/92$03.00 1992©IEEE

is based on the purpose of the task, shape and size of the object, and the posture of the fingers. This division of grasps into precision and power grasps is the most widely accepted and used by researchers in the medical, biomechanical and robotic fields. A power grasp is used for higher stability and security at the expense of object maneuverability, while the converse is true for a precision grasp. A precision grasp is characterized by a small degree of contact between the hand and the object. In this type of grasp, the object is normally pinched between the thumb and the flexor aspects of at least one finger. In a power grasp, however, the object is held tight by the fingers and the palm[1]. The major classifications of a power grasp are the cylindrical power grasp and the spherical power grasp. In a cylindrical power grasp, the thumb can either be adducted for some element of precision, or abducted[2] for more clamping action on the object. Henceforth the cylindrical power grasp refers to the former type while the "coal-hammer" grasp refers to the latter type.

Cutkosky and Wright [11] construct a hierarchical tree of grasps beginning with Napier's distinction between precision and power grasps. At the lowest level, a grasp is chosen (either by the human or the computer) based on object geometric details and task requirements.

In our effort to automate the recognition of grasps, we require a grasp taxonomy which could provide a systematic way of identifying grasps based on the hand configuration and object shape. We propose a grasp taxonomy based on the analysis of the effective contact points of the hand with the grasped object. The effective contact point of a finger segment represents the surface contact of that segment with the object. The resultant spatial pattern of contact points forms what we call a *contact web*.

2.2 The Contact Web

2.2.1 Definitions

A *contact web* is defined as a 3-D graphical structure connecting the effective points of contact between the hand and the object grasped. When parts of a finger or palm make contact with the grasped object, the actual contact area is finite. A point contact is useful in conceptually representing the contact between the phalangeal segments and palm[3], and the object because of ease of representation and analysis, and accommodation of uncertainty in grasping. The shape and cardinality of the contact web yield important information about the type of grasp effected.

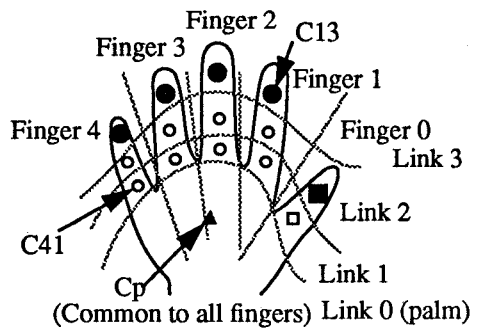

Fig. 1 **Contact Notation on the right hand (palmar side)**

Intradigital contact points are contact points along the same finger. *Interdigital contact points* are those located at different fingers. The contact notation adopted is illustrated in Fig. 1.

P_I^i is the intradigital contact point set for the ith finger ($i = 0$ (the thumb), 1, 2, 3, 4);

E.g., $P_I^1 = \{C_{13}\}$ refers to the finger tip contact point set of the index finger.

$P_C = \{\text{fingers in contact with object}\}$;

$P_H = \{ P_I^i : i \in P_C \}$ (the contact point set);

$N_0(P_H)$ = cardinality of P_H = number of fingers in contact with object;

$$N_1(P_H) = N_0\left(\bigcup_{i \in P_C} P_I^i\right) = \text{total number of contact points.}$$

Note: $N_1(P_H)\big|_{max} = 15.$

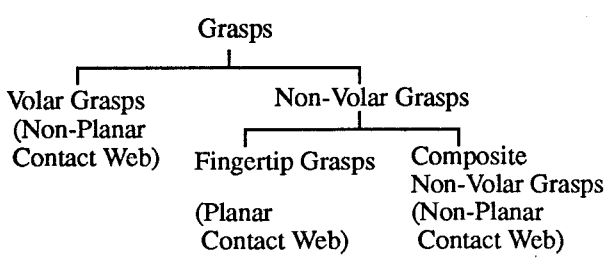

Fig. 2 **Major classifications of grasps for recognition**

2.2.2 A Taxonomy based on the Contact Web

We propose a grasp taxonomy which is based on the contact web. It provides a systematic way of recognizing grasps from the hand configuration and the object shape. In addition, it provides a more continuous classification of grasps by not restricting the classification to discrete grasp groups.

1. An exception is the lateral pinch, which is the grasp employed when turning a key in a lock. This grasp involves the thumb and the radial side of the index finger.

2. When the thumb is adducted, it lies more or less on the plane of the palm; it subtends an angle with the plane of the palm when it is abducted.

3. Note that the contact point of the palm is merely an artifact which represents the effective contact of the palm with the grasped object. This point may of may not be physically in contact with the object.

A power grasp is characterized by a high degree of contact between the hand and the held object. This allows high clamping forces on the object. A feature that we use to first distinguish between grasps is the involvement of the palm surface in the grasp. Grasps which involve the palm surface are called *volar grasps* while others are called *non-volar grasps*. All volar grasps are power grasps. All but one type of non-volar grasps are precision grasps[4]. The exception mentioned is the lateral pinch, which is the grasp assumed by the hand when turning a key in a lock. The non-volar grasps are further classified as *fingertip grasps* and *composite non-volar grasps*. The fingertip grasp involves only the fingertips while the composite non-volar grasp involves surfaces of other segments of the fingers in addition to the fingertips. The major grasp classifications are shown in Fig. 2, while the effective contact point notation is depicted in Fig. 1.

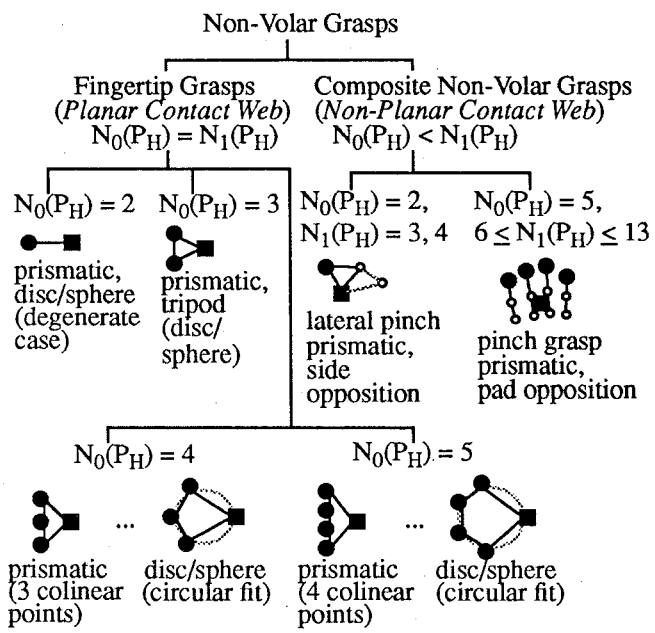

Fig. 3 **Classification of non-volar grasps**

One interesting feature of this category of grasps is whether the contact web associated with that category is planar or non-planar. The contact web formed by a volar grasp is spatially non-planar (except for the platform push[5]). In most non-volar grasps where the areas of contact between the object and the hand are those of the fingertips (fingertip grasps), the associated contact web is approximately planar. However, there are at least two identifiable cases of non-volar grasps where the contact web is non-planar, namely the lateral pinch and the pinch grasp. These are separately grouped as composite non-volar grasps.

The contact web enables a more continuous categorization of grasps as shown in Fig. 3 and Fig. 4. The degree of membership to a strictly prismatic grasp or spherical/disc grasp lies in the degree of fit of the contact points to the respective shapes. In addition, the contact web facilitates a mathematical framework for the recognition of grasps as described in Subsection 2.4. This grasp taxonomy also provides a systematic means of grasp discrimination from observation.

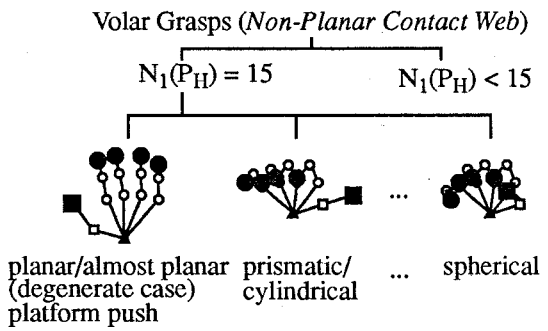

Fig. 4 **Classification of volar grasps**

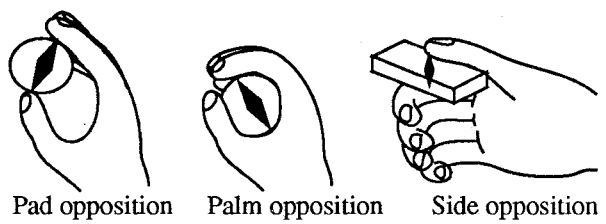

Fig. 5 **Types of opposition (adapted from [16])**

2.3 Virtual Fingers and Opposition Space

By analyzing the contact web, medium level grasp concepts such as virtual fingers and opposition space, can be described. These two concepts, in turn, are the key elements in characterizing the type of grasp and indicating the functionality of the grasp.

Arbib et al. [13] introduced the concept of the virtual finger: a functional unit comprised of at least one real physical finger (which may include the palm). The real fingers comprising a virtual finger act in unison to apply an opposing force on the object and against the other virtual fingers in a grasp. This concept replaces the analysis of the mechanical degrees

4. Napier [17] regards volar grasps as power grasps and non-volar grasps as precision grasps. This view is shared by various other researchers in the medical and biomechanical fields (e.g., [19], [20]). However, this would not be *strictly* true if we adhere to the position that the type of grasp should be classified according to the predominance of either power or precision in the grasp (which, interestingly, Napier [17] adheres to as well). The demand for power is higher than the demand for precision in the lateral pinch; though it is a non-volar grasp, it is, by the power predominance definition, a power grasp.

5. The platform push is a *non-prehensile* grasp; non-prehensile grasps are not considered in this work.

of freedom of individual fingers by the analysis of the functional roles of forces being applied in a grasp [13].

Iberall et al. [14] define opposition space as "the area within the coordinates of the hand where opposing forces can be exerted between virtual finger surfaces in effecting a stable grasp." They show that prehensile grasps involve combinations of the three basic oppositions shown in Fig. 5. Opposition space is an important concept in characterizing grasps.

2.4 Recognizing Grasps from the Contact Web

We now illustrate how the contact web can be used to identify the grasp. We start with the simplest type of opposition, namely, pad opposition, and then proceed to side opposition. The detailed analyses involving these oppositions in the next two subsections constitute the main ideas that embody the mathematical framework for grasp recognition. Note that these analyses are done from the geometrical perspective. This is motivated by the fact that humans classify a grasp irrespective of the hand orientation and without explicit static analysis of the grasp.

2.4.1 Pad Opposition Only

There are at least two virtual fingers to effect this opposition. The *degree of coupling* between any two given contact normals $\mathbf{n}_i$ and $\mathbf{n}_j$ is defined to be their normalized dot product:

$$D_c(i,j) = \frac{\mathbf{n}_i \bullet \mathbf{n}_j}{|\mathbf{n}_i||\mathbf{n}_j|}$$

The following is a proposed analytical method of determining the mapping of all the fingers touching the grasped object into either one, two or three virtual fingers. Note that this method does not presume the mapping of the thumb into one virtual finger.

The *virtual finger membership index* between fingers i and j (each with only one contact point for the moment) is defined as:

$$m_{ij} = \frac{\min(|\mathbf{n}_i|, |\mathbf{n}_j|)}{\max(|\mathbf{n}_i|, |\mathbf{n}_j|)} \frac{1 + D_c(i,j)}{2}$$

It can be seen that $0 \le m_{ij} \le 1$. Two real fingers are more likely to be members of the same virtual finger if the contact normals are similar. Obviously $m_{ii} = 1$ and $m_{ij} = m_{ji}$. Let VF_k denote the set of real fingers hypothetically belonging to the kth virtual finger. Then the *cohesive index* for that virtual finger is defined as the geometric mean of all the pairwise virtual membership indices:

$$C_{VF,k} = \prod_{\substack{i,j \in VF_k \\ j \ge i}} m_{ij}^{\xi}$$

where $$\xi = \binom{N(VF_k)}{2}^{-1}$$

$N(VF_k)$ being the number of real fingers in virtual finger VF_k and ξ is the reciprocal of the number of possible pairs of real fingers in virtual finger VF_k. $C_{vf,k}$ characterizes the similarity of action of the real fingers in VF_k. If all the fingers in VF_k act in unison, i.e., the contact normals are equal, then $C_{vf,k} = 1$. However, if any two fingers in VF_k possess anti-parallel contact normals, then $C_{vf,k} = 0$.

The problem of determining the number of virtual fingers and the constituents of each virtual finger can be described as a non-linear mixed program:

$$\text{Maximize} \quad C_{eff} = \left(\frac{1}{n_{VF}!} \prod_{i=1}^{n_{VF}} C_{VF,i}\right)^{\frac{1}{n_{VF}}}$$

$$\text{subject to} \quad n_{VF} \in \{1, 2, 3\}$$

$$\bigcup_{i=1}^{n_{VF}} VF_i = RF$$

$$VF_i \cap VF_j = \varnothing, \qquad i \ne j; \qquad (1 \le i, j \le n_{VF})$$

The product term with the exponent in the objective function C_{eff} is the geometric mean of the membership indices of the hypothesized virtual fingers. This ensures that the division of real fingers into virtual fingers is done in such a way that the real fingers in each virtual finger act on the object in as similar a manner as possible. C_{eff} is called the *grasp cohesive index*. The remaining factor in the objective function is a contrived one to favor a smaller number of virtual fingers should there exist equivalency in the objective function (without this factor) for different hand configurations comprising different numbers of virtual fingers. RF is the set of real fingers in contact with the grasped object.

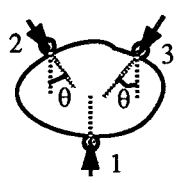

(a) $\theta = 30^o$	(b) $\theta = 50^o$
$m_{12} = 0.07$	$m_{12} = 0.18$
$m_{13} = 0.07$	$m_{13} = 0.18$
$m_{23} = 0.75$	$m_{23} = 0.41$

Fig. 6 **Illustration for Example (a) and (b)**

In the example shown in Fig. 6, the object held roughly resembles an ellipse. For case (a), the highest value for C_{eff} is obtained for $VF_1 = \{1\}$ and $VF_2 = \{2, 3\}$ (here $C_{eff,max} = 0.612$). However, in case (b), the highest value for C_{eff} is obtained for $VF_1 = \{1\}$, $VF_2 = \{2\}$, and $VF_3 = \{3\}$ ($C_{eff,max} = 0.550$). (Note that θ is the angle measured with respect to the vertical line to which the contact normal at point 1 is anti-parallel.)

2.4.2 Side Opposition Only

Side opposition involves two fingers, e.g., the thumb and the index finger. Contact points that are part of the same finger (i.e., intradigital contact points) are automatically grouped together. This means that either one or two virtual fingers exist in this type of grasp configuration. The kth "composite" finger comprising ℓ ($\ell = 2$ or 3) intradigital contact points is denoted by $k \rightarrow \{1, ..., \ell\}$. The mixing rule employed for the "composite" finger is

$$m_{i,j \rightarrow \{1,...,\ell\}} = \frac{1}{2}\left(\prod_{p=1}^{\ell} m_{i,j \rightarrow p} + \max_{p \in \{1,...,\ell\}} m_{i,j \rightarrow p}\right)$$

and an example of how the mixing rule is used is shown in Fig. 7.

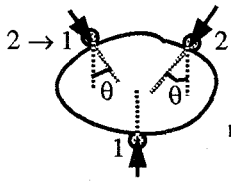

$$\theta = 30^{o}$$
$$m_{1,2 \rightarrow 1} = 0.07$$
$$m_{1,2 \rightarrow 2} = 0.07$$
$$m_{1,2 \rightarrow \{1,2\}} = \frac{1}{2}(4.9 \times 10^{-3} + 0.07) = 0.0375$$

Fig. 7 **Illustration for mixing rule application**

2.4.3 Hand Configuration Notation

A shorthand notation for the configuration of the hand, say, $VF_1 = \{1\}$, $VF_2 = \{2, 3, 4\}$ is $\{(1)(234)\}$. This notation will be used in the remainder of this paper.

2.4.4 General Mixing Rule for "Composite" Fingers

The virtual finger membership index between two "composite" fingers i and j is given by the expression

$$m_{i \rightarrow \{1,...,\ell_i\}, j \rightarrow \{1,...,\ell_j\}} = \frac{1}{2}\left(\prod_{q=1}^{\ell_j} \max_{p \in \{1,...,\ell_i\}} m_{i \rightarrow p, j \rightarrow q} + \prod_{p=1}^{\ell_i} \max_{q \in \{1,...,\ell_j\}} m_{i \rightarrow p, j \rightarrow q}\right)$$

The expression on the right is easily seen to be commutative in "composite" fingers i and j, and it reduces to the equation in Subsection 2.4.2 when $\ell_i = 1$. If the two "composite" fingers are fully compatible, i.e., $\ell_i = \ell_j = \ell$ (say) and $m_{i \rightarrow p, j \rightarrow q} = 1$ for p, q = 1, ..., ℓ, then $m_{i \rightarrow \{1,...,\ell_i\}, j \rightarrow \{1,...,\ell_j\}} = 1$, as to be expected.

3.0 Experiments and Results

3.1 Analysis of Grasps by Human Subjects

The details of the experiments conducted to illustrate the use of the mathematical framework for both precision and power grasps are given in [22]. In summary, while there is some link of the effective cohesive index to the type of non-volar grasp, it is not sufficient to identify it. On the other hand, there is a marked trend in the effective cohesive index with respect to the volar grasp. The index, as expected, decreases from a cylindrical grasp to a spherical grasp. Another interesting feature of the results is that the index varies very little with the change in the radius of the circular cross-section of the cylinder grasped. In addition, the index did not change much when a cylinder with different elliptical cross-sections were used.

3.2 Procedure for Grasp Recognition

Using the results of a series of experiments conducted [22], a grasp can be identified from the following general steps:

1. *Compute the real finger to virtual finger mapping which yields the virtual finger compositions and the grasp cohesive index.*
2. *If the palm surface is not involved in the grasp, classify it as a non-volar grasp.*
3. *Otherwise, by checking the grasp cohesive index and, if necessary, the degree of thumb abduction, classify it either as a spherical, cylindrical or coal-hammer (type 1 or type 2) power grasp.*

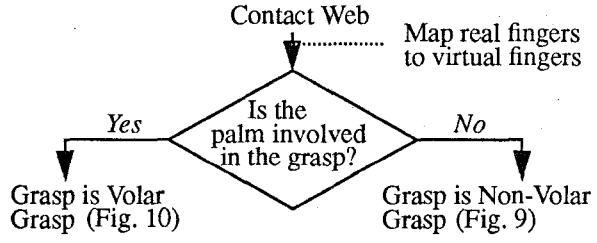

Fig. 8 **Recognition of major type of grasp**

A grasp can be classified as a volar grasp or non-volar grasp according to whether there is volar-object interaction or not (Fig. 8). If it is a non-volar grasp, further classification can be done by checking if only the fingertips are involved in the grasp, and the contact points' closeness of fit to a circle or rectangle. This is illustrated in Fig. 9. Unless the grasp is a lateral pinch (in which case the grasp is a power grasp), the grasp is classified as a precision grasp.

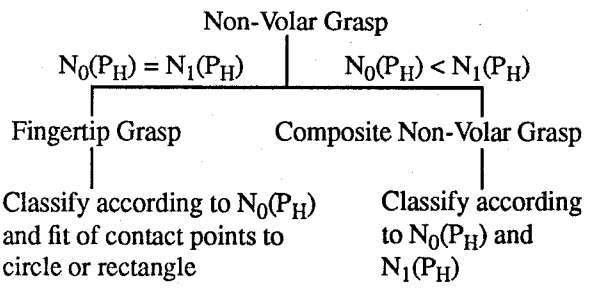

Fig. 9 **Discrimination graph for non-volar grasps**

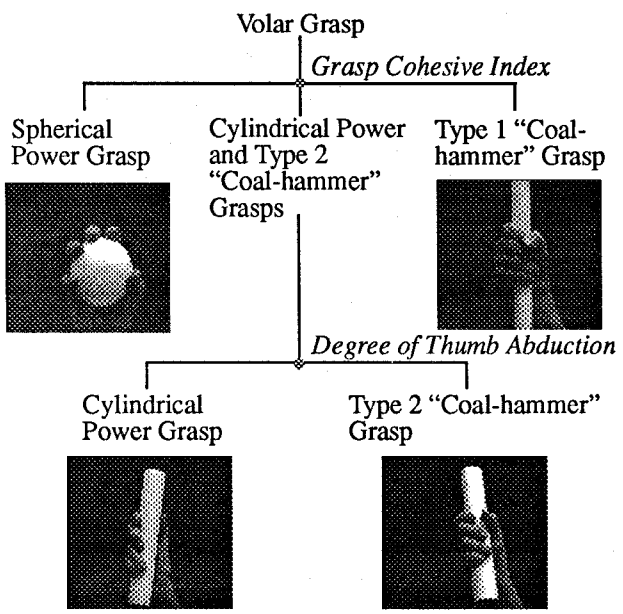

Fig. 10 **Discrimination graph for power grasps**

The volar grasp discrimination procedure in step 3 is graphically depicted in Fig. 10. The "coal-hammer" grasp is a special case of the cylindrical power grasp, and is identified by the high degree of thumb abduction. We define the type 1 "coal-hammer" grasp to be one in which the thumb does not touch the held object, while the type 2 "coal-hammer" grasp refers to one in which the thumb touches the object. (Note that all volar grasps are power grasps.) The first level of classification is performed using the following discrimination function:

$$\tau_i = e^{-\frac{1}{2}\left(\frac{x-\mu_i}{\sigma_i}\right)^2}$$

where μ_i is the mean value of the grasp cohesive index for the ith power grasp category and σ_i is the associated standard deviation. The power grasp category is identified by the largest value of the discrimination function. Should the cylindrical and type 2 "coal-hammer" grasps need to be discriminated, we would then determine the degree of thumb abduction. The type 2 "coal-hammer" grasp is associated with a high degree of thumb abduction.

Note that the object shape has not been directly taken into consideration here; the local object shape (i.e., part of the object within the compass of the hand) has been implicitly taken care of by the contact web.

3.3 Grasp Recognition from Range and Intensity Images

Two range and intensity image sequences of finger movements leading to different power grasps were taken and then analyzed using the grasp recognition scheme described earlier. In each sequence, the fingers are tracked to the final grasp configuration before the grasp is identified. However, prior to this, the hand model needs to be initialized. This is done using a separate program.

3.3.1 Hand Model Initialization

Each finger segment is modeled by a cylinder. The purpose of the hand model initialization is to determine the finger segment cross-sectional radius and length, and the relative positions of the fingers. The assumed hand posture is with the fingers fully extended, and such that the plane of the palm is approximately perpendicular to the camera viewing direction. These fingers are taken to be the reference positions, and abduction angles are measured relative to these positions.

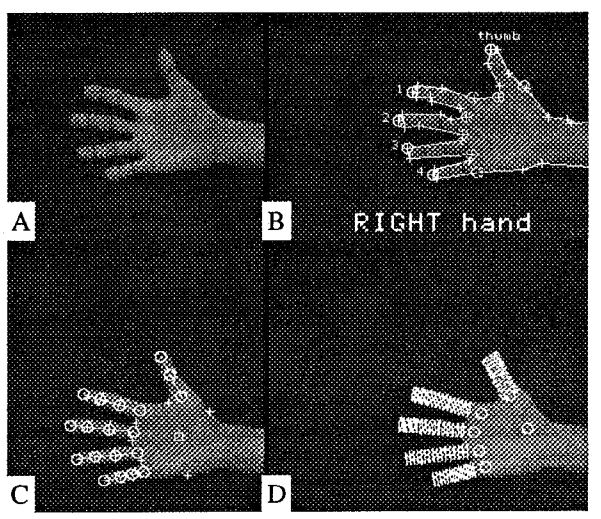

Fig. 11 **Hand model initialization. A. Intensity image; B. Identification of fingers; C. Localization of finger joints; D. Cylindrical fitting of fingers.**

In addition, to facilitate the measurement of finger segment lengths, dark lines were drawn across the finger at the distal and proximal interphalangeal joints (except for the thumb, where a dark line was drawn across it at the interphalangeal joint). The proximal finger segment length is calculated from

empirical anthropometric studies of human finger segment length ratios [8].

The steps involved in hand model initialization are:

1. *Thresholding and hand boundary extraction*
2. *Curvature analysis of hand boundary to detect fingertips and grooves between fingers*
3. *Identification of finger regions according to inter-finger distances*
4. *Location of interphalangeal joints using the Hough transform and calculation of finger segment lengths*
5. *Determination of best fit cylinders from range data*

Fig. 11 shows the intensity image of a hand and three snapshots of the hand model initialization program.

3.3.2 Finger Tracking

The basic method used in finger tracking is local search of the minimum sum of two types of matching errors: error in range data fitting, and error in matching the hypothesized finger 2-D projection to the actual finger position in the image. While tracking the fingers, limits of the finger joint angles which are consistent with anatomical and physiological studies of the hand (e.g., [7], [8], and [9]) are imposed. One main assumption made is that the hand does not move; only the fingers move (via flexion, extension, abduction and adduction).

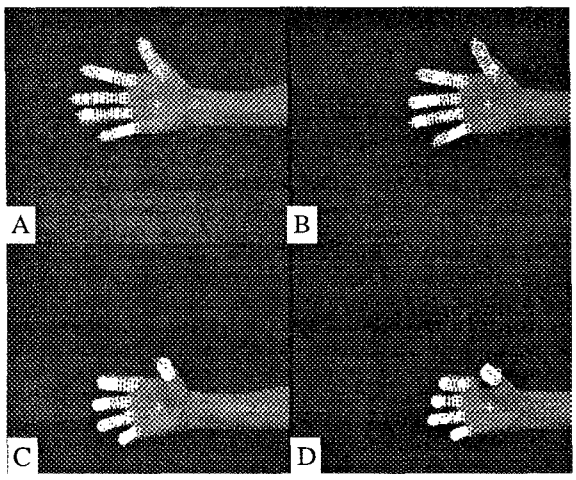

Fig. 12 **Finger tracking sequence for Ex. 1: A. Frame 1; B. Frame 3; C. Frame 6; D. Frame 8**

3.3.3 Grasp Recognition Results

The results of the analysis of two sets of range and intensity images are shown in this subsection. The first example is shown in Fig. 12 and Fig. 13. Four of the eight frames for this grasp sequence is shown in Fig. 12. The second example is shown in Fig. 14.

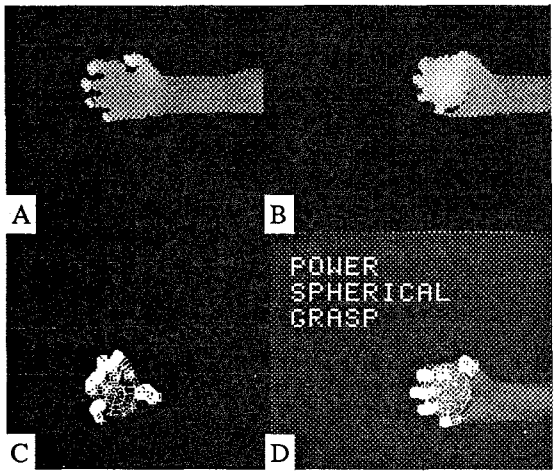

Fig. 13 **Recognition results for a spherical power grasp. A. Range image of last frame of sequence; B. Range image of hand and object; C. Alternate view of tracked fingers with object; D. Classification of grasp**

The grasp cohesive index for the first example (Fig. 13) is 0.356, with the following virtual finger compositions: $VF_1 = \{0\}$, $VF_2 = \{1\}$, and $VF_3 = \{2, 3, 4, 5\}$. This grasp is classified as a spherical power grasp.

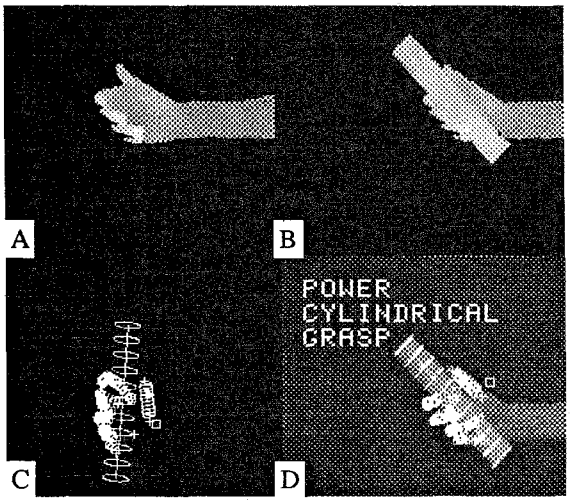

Fig. 14 **Recognition results for a cylindrical power grasp. A. Range image of last frame of sequence; B. Range image of hand and object; C. Alternate view of tracked fingers with object; D. Classification of grasp**

The grasp cohesive index for the second example (Fig. 14) is 0.508, with the following virtual finger compositions: $VF_1 = \{0\}$, $VF_2 = \{1\}$, and $VF_3 = \{2, 3, 4, 5\}$. From the grasp cohesive index, this grasp can either be a cylindrical power or type 2 "coal-hammer" grasp. Since the angle of the thumb

subtends only 23° with the standard (original) thumb posture, it is classified as a cylindrical power grasp.

The experiments and their results described in [22] and Subsection 3.3 indicate that it is possible to categorize grasps by using the contact web and real finger to virtual finger mapping. This mapping is instrumental in characterizing the type of grasp demonstrated in the scene.

4.0 Conclusions

A framework for recognizing a grasp has been described in this paper. A 3-D structure comprising a network of effective contact points of the hand with the grasped object is proposed as a tool for grasp analysis. We call this 3-D structure the *contact web*. It enables the grasp to be classified in a more continuous manner. In addition, by employing a particular real finger to virtual finger mapping, the grasp can be described in higher level conceptual terms such as virtual finger composition and opposition space. Another important consequence of this mapping is an index called the *grasp cohesive index*, which can be used to identify the grasp.

The grasp is one of the three identifiable phases in a grasping task. The other two phases are the pre-grasp and manipulation phases. Future work will be devoted to the analysis of these two phases in our effort to automate the recognition of a grasping task. All this is in line with the Assembly Plan from Observation (APO) paradigm, which epitomizes the capability of a robotic system to replicate a task by observing and understanding the same task performed by a human operator.

Acknowledgments

We would like to thank Kathryn Porsche and Fred Solomon for proofreading drafts of this paper. The verification of our proposed framework for grasp recognition has been made possible by the gracious participation of the numerous volunteers in our grasping experiments. We really appreciate their help. We would also like to thank George Paul for helping us take some of the images used in this paper.

References

[1] P. Lammineur, and O. Cornillie, *Industrial Robots*, Pergammon Press, 1984, pp. 43-54.

[2] H. Asada, and Y. Asari, "The direct teaching of tool manipulation skills via the impedance identification of human motions," *Proc. IEEE Int'l Conf. on Robotics and Automation*, 1988, pp. 1269-1274.

[3] R. Finkel, R. Taylor, R. Bolles, R. Paul, and J. Feldman, "*AL: A Programming System for Automation*," Tech. Rep. AIM-177, Stanford University, Artificial Intelligence Lab., 1974.

[4] T. Lozano-Perez, "Automatic planning of manipulator transfer movements," *IEEE Trans. on Systems, Man and Cybernetics*, SMC-11(10), 1981, pp. 681-689.

[5] K. Ikeuchi, and T. Seuhiro, "Towards an Assembly Plan from Observation: Task recognition with polyhedral objects," *CMU Tech. Rep. CMU-CS-91-167*, Aug. 1991.

[6] T. Kuniyoshi, M. Inaba, and H. Inoue, "Teaching by showing: Generating robot programs by visual observation of human performance," *Proc. 20th Int'l Symp. on Industrial Robots*, 1989, pp. 119-126.

[7] *Joint Motion: Method of Measuring and Recording*, American Academy of Orthopedic Surgeons, Chicago, 1965.

[8] K.N. An, E.Y. Chao, W.P. Cooney, and R.L. Linscheid, "Normative model of human hand for biomechanical analysis," *Journal of Biomechanics*, vol. 12, 1979, pp. 775-788.

[9] C.L. Taylor, and R.J. Schwarz, "The anatomy and mechanics of the human hand," *Artificial Limbs*, no. 2, 1955, pp. 22-35.

[10] G. Schlesinger, "Der mechanische aufbau der kunstlichen glieder," Borchardt, et al. (eds.), *Ersatzglieder und Arbeitshilfen fur Kriegsbeschadigte und Unfallverletzte*, Springer, 1919, pp. 321-699.

[11] M.R. Cutkosky, and P.K. Wright, "Modeling manufacturing grips and correlations with the design of robotic hands," *Proc. IEEE Int'l Conf. on Robotics and Automation*, 1986, pp. 1533-1539.

[12] M.R. Cutkosky, "On grasp choice, grasp models and the design of hands for manufacturing tasks," *IEEE Trans. on Robotics and Automation*, 5(3), 1989, pp. 269-279.

[13] M.A. Arbib, T. Iberall, and D.M. Lyons, "Coordinated control programs for movements of the hand," *Hand Function and the Neocortex*, eds. Goodwin, A.W., and Darian-Smith, I., Springer-Verlag, 1985, pp. 111-129.

[14] T. Iberall, G. Bingham, and M.A. Arbib, "Opposition space as a structuring concept for the analysis of skilled hand movements," *Experimental Brain Research Series 15 - Generation and Modulation of Action Patterns*, eds. Heuer, H., and Fromm, C., Springer-Verlag, 1986, pp. 158-173.

[15] T. Iberall, "The nature of human prehension: Three dextrous hands in one," *Proc. IEEE Int'l Conf. of Robotics and Automation*, 1987, pp. 396-401.

[16] T. Iberall, and C.L. MacKenzie, "Opposition space and human prehension," *Dextrous Robot Hands*, eds. Venkataraman, S.T., and Iberall, T., Springer-Verlag, 1990, pp. 32-54.

[17] J. Napier, "The prehensile movements of the human hand," *Journal of Bone and Joint Surgery*, vol. 38B, no. 4, 1956, pp. 902-913.

[18] D.M. Lyons, "A simple set of grasps for a dextrous hand," *Proc. IEEE Int'l Conf. on Robotics and Automation*, 1985, pp. 588-593.

[19] B. Buchholz, and T.J. Armstrong, "A kinematic model of the human hand to evaluate its prehensile capabilities," to appear in *Journal of Biomechanics*, vol. 25, 1991.

[20] C. Long, P.W. Conrad, E.A. Hall, and S.L. Furler, "Intrinsic-extrinsic muscle control of the hand in power grip and precision handling," *Journal of Bone and Joint Surgery*, vol. 52-A, no. 5, 1970, pp. 853-867.

[21] K. Ikeuchi, and M. Hebert, "Task oriented vision," *CMU Tech. Rep. CMU-CS-91-163*, July 1991.

[22] S.B. Kang, and K. Ikeuchi, "A framework for recognizing grasps," *CMU Tech. Rep. CMU-RI-TR-91-24*, Nov. 1991.